

Influence of the distance on the interaction between an autonomous pacemaker and a reentry

M. deCastro,* M. Gómez-Gesteira, and V. Pérez-Villar

Group of Nonlinear Physics, Faculty of Physics, University of Santiago de Compostela, 15706 Santiago de Compostela, Spain

(Received 10 March 1997; revised manuscript received 22 July 1997)

An experimental reentry was generated in a two-dimensional array of electronic cells to study the influence of the distance on the interaction between that reentry and an external and autonomous pacemaker. For long distances ($d \geq 2/3\lambda$, where λ is the reentry wavelength), the pacemaker is only able to modify the rhythm of the medium for periods faster than the reentry period. For shorter distances ($d < 2/3\lambda$), the pacemaker is able to modify the rhythm of the medium even for periods slower than the reentry period, giving rise to complex sequences of multiperiod output waves when both pacemakers are close enough. [S1063-651X(98)06001-2]

PACS number(s): 87.90.+y, 07.50.Ek, 84.30.-r, 05.45.+b

I. INTRODUCTION

In some periodically active biological systems [1,2], the rhythm of the medium is set by specialized cells called pacemakers that periodically discharge, starting a wave of excitation that spreads throughout the medium. Under certain conditions, it is possible to initiate a ‘‘reentrant path’’ of excitation in which a wave travels in a closed path. In cardiac tissue, this is believed to be the origin of some pathologies known as tachycardias [3–6]. In such a case, the period of this reentrant excitation, if it persists, is usually faster than the normal one and generates an abnormal pacemaker called an ‘‘ectopic pacemaker.’’ The behavior of this reentrant excitation has been studied in two-dimensional excitable media [1,7–10] and in a ring [9,11,12].

The existence and competition between different frequencies have been analyzed from different points of view, in both oscillatory and excitable media. Some authors have studied the response of a single cell [13–16] and of an extended medium [15–19] to a periodic forcing both numerically and experimentally. They have observed phase locking, aperiodic rhythms with typical sequences corresponding to devil’s staircase and Farey tree [20,21], and, even, low dimensional chaos. Competition between two wave sources has been widely analyzed experimentally in chemical [22–26] and electronic media [27,28] and numerically [29] and theoretically in reaction-diffusion systems [30]. In cardiac tissue, Courtemanche *et al.* [31] have studied the interaction between a normal pacemaker and an ectopic one by circle map techniques. In most of these references, the distance between sources was not explicitly considered; in fact, only Refs. [23,24] considered the distance to play a key role in spiral interaction.

The aim of this paper is to generate and characterize a reentrant path in a two-dimensional array of electronic cells, which plays the role of an ectopic pacemaker, and to analyze the influence of distance on the interaction between an autonomous and external pacemaker and that reentry. In Sec. II the experimental setup is described. In Sec. III a reentry is created and its properties are characterized. In Sec. IV the influence of distance on the reentry-pacemaker interaction is

analyzed. The results obtained show that for long distances ($d \geq 2/3\lambda$, where λ is the reentry wavelength), the pacemaker is only able to modify the rhythm of the medium for $T_p < T_r$ and for shorter distances ($d < 2/3\lambda$) the pacemaker is able to modify the rhythm of the system even for $T_p > T_r$. The particular case of nearby sources, where complex multifrequency output waves are obtained, is especially studied in Sec. V. In this case, a devil’s staircase is calculated for two different output frequencies. All results are discussed in Sec. VI.

II. EXPERIMENTAL SETUP

The experimental setup, represented in Fig. 1(a), consists of two linear arrays of 45 nonlinear circuits. All cells [32–34] are similar within the limits allowed by commercial tolerances (1%) and exhibit an excitable behavior for the following values of its parameters: $C_1 = 1$ nF, $L = 10$ mH, $R_{\text{int}} = 270$ Ω , $C_2 = 12$ nF, $r_0 = 10$ Ω .

Each cell is longitudinally coupled with its neighbors by a resistance R_l and transversally with the opposite cell in the other array through a higher resistance R_t . An obstacle was created in the middle of the arrays by uncoupling transversally some circuits. Longitudinal resistances on both sides of the obstacle were considered to be different. Thus, in the first array (the one on the left), some consecutive circuits were longitudinally coupled by a high resistance ($R_o = 1$ M Ω) connected in parallel with a buffer and a resistance R_l as shown in Fig. 1. This allows normal wave propagation upward, but prevents it downward due to propagation failure [35,36]. This setup mimics some of the properties experimentally observed in cardiac muscle as the presence of an obstacle of unexcitable tissue and directional properties of propagation around it [37,38]. Finally, the first cells in both arrays were connected to a pulse generator, which was externally controlled to deliver a pulse or a wave train of upper-threshold amplitude (4.5 V). The measuring points were located at the end of both arrays.

III. REENTRY GENERATION AND DESCRIPTION

To generate an experimental reentry, a single pulse was delivered, giving rise to a wave propagating downward in both arrays. When a wave arrives at the obstacle, it starts

*Electronic address: uscfmmcr@cesga.es

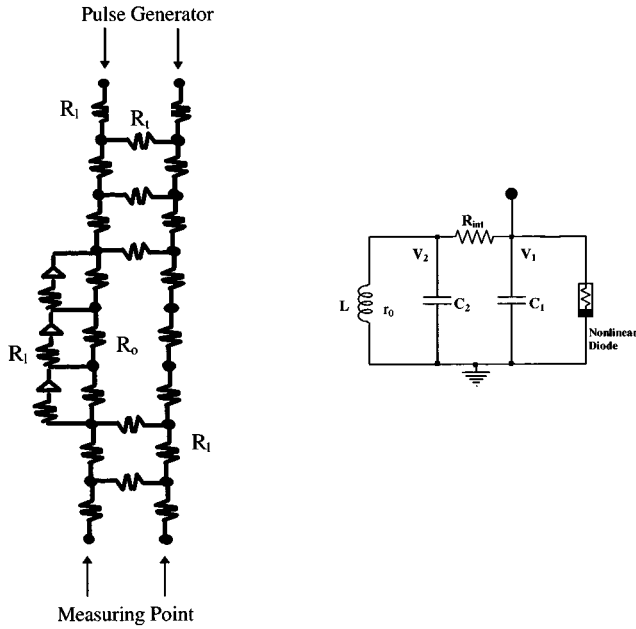


FIG. 1. Experimental setup consisting of two linear arrays of 45 cells. Each cell (plotted on the right) is connected to the black spots through the node V_1 , and coupled with its nearest neighbors (longitudinally by resistances R_l and transversally by R_t with $R_l < R_t$). An obstacle was generated in the middle of the arrays by uncoupling transversally some circuits. Longitudinal resistances on both sides of the obstacle were considered to be different. In the array on the left, circuits were longitudinally coupled with a high resistance ($R_0 = 1 \text{ M}\Omega$) connected in parallel with a buffer and a resistance R_l . This allows normal propagation upward, but prevents it downward. The first cells in both arrays were connected to a pulse generator. Circuit parameters: $C_1 = 1 \text{ nF}$, $L = 10 \text{ mH}$, $R_{\text{int}} = 270 \Omega$, $C_2 = 12 \text{ nF}$, $r_0 = 10 \Omega$ correspond to an excitable behavior.

propagating on both sides, but it is stopped in the first array due to propagation failure. So, when the wave propagating through the second array reaches the end of the obstacle, it splits into two, one of them spreading downward and the other one transversally to the other array. There, the wave splits once again into two waves moving downward and upward. If the obstacle is big enough, each cell in the first array can recover itself after the spread of the last excitation and allow the propagation of the next wave. So, a reentry can be formed and remain stationary. In this way, it is possible to obtain an infinite number of responses (output waves) to a single stimulus (input wave).

To illustrate this process, a reentry was generated in two linear arrays with $R_l = 2.3 \text{ k}\Omega$ and $R_t = 4.7 \text{ k}\Omega$. With these values there is some critical T value ($T_m = 110.0 \pm 0.5 \mu\text{s}$) below which the system is unable to sustain a wave for every pulse delivered by the generator. This will be considered the refractory period of the medium. A two-dimensional plot of this reentry (30 circuits long—15 in each array—and a period of $T_r = 178.0 \pm 0.5 \mu\text{s}$, obstacle size is considered to be the reentry wavelength) is shown in Fig. 2(a) at three different times. The black strips represent the peak of the wave, and the central line the region without transversal connections (obstacle). Waves outside the reentry were not plotted for the sake of clarity. Figure 2(b) shows the linear increase of the reentry period with the number of cells in the obstacle.

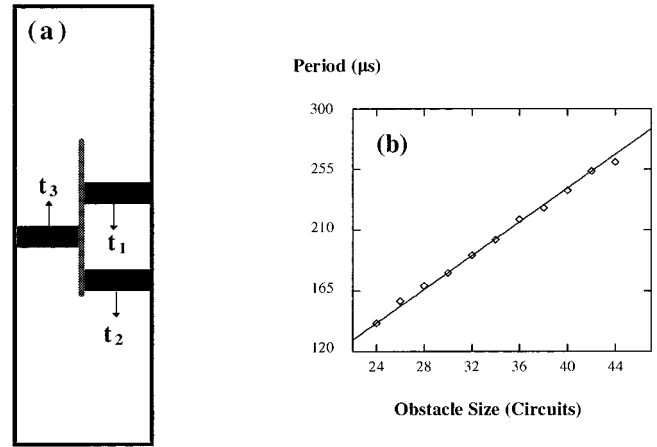


FIG. 2. (a) Two dimensional plot of an experimental reentry (30 circuits—15 in each array—long and a period of $T_r = 180.0 \pm 0.5 \mu\text{s}$) measured at three different times ($t_1 = 60 \mu\text{s}$, $t_2 = 90 \mu\text{s}$ and $t_3 = 120 \mu\text{s}$) after the passage of the wave through the first cell of the obstacle. The black strips represent the peak of the wave, and the central line the obstacle (region without transversal connection). The clockwise movement of the reentry is marked by the arrows. Waves outside the reentry were not plotted for the sake of clarity. (b) Linear increase of the reentry period with the size of the obstacle.

IV. INFLUENCE OF THE DISTANCE ON REENTRY-PACEMAKER INTERACTION

A reentry with a period of $T_r = 330 \pm 2.5 \mu\text{s}$ is considered in two linear arrays with $R_l = 4.7 \text{ k}\Omega$ and $R_t = 5.6 \text{ k}\Omega$ to study its interaction with a wave train of period T_p delivered by the pulse generator. One pulse produces the formation of a reentry around the obstacle (the size of the obstacle is considered to be the reentry wavelength, $\lambda = 30$). We have observed that the obstacle is big enough to support two waves traveling around it in a stationary way. Thus, the rest of the pulses interact with this reentry, giving rise to different sequences of output waves measured far from the obstacle region. These output waves can have one or several frequencies depending on the relation between T_p and T_r (we will consider $T_p \in [T_m, 2T_r]$).

The distance between the reentry and the autonomous and external pacemaker is an important factor that affects the interaction between them. When the distance between both pacemakers is long enough, $d \geq 2/3\lambda$ (Fig. 3), for $T_p > T_r$ the reentry dominates and imposes its rhythm on the medium. For values of $T_p \in [T_r - T_m, T_r]$ the normal pacemaker dominates the rhythm of the medium. This behavior changes for values of $T_p \in (T_r/2, T_r - T_m)$, where output waves with two different periods were obtained as a result of the interaction between both sources ($T_1 = T_m = 110 \pm 2.5 \mu\text{s}$ and $T_2 = 220 \pm 2.5 \mu\text{s}$, following the sequence $T_1 T_2$, with $T_1 + T_2 = T_r$). Finally, for $T_p \leq T_r/2$ the pacemaker dominates again.

For intermediate distances, $d \in [1/3\lambda, 2/3\lambda]$ (Fig. 4), there exists an interaction between both pacemakers even for $T_p > T_r$. A two period sequence ($T_1 T_2$ with $T_1 = T_m = 110 \pm 2.5 \mu\text{s}$ and $T_2 = 220 \pm 2.5 \mu\text{s}$) is observed. For $T_p \in [T_r - T_m, T_r]$ the pacemaker dominates and imposes its rhythm

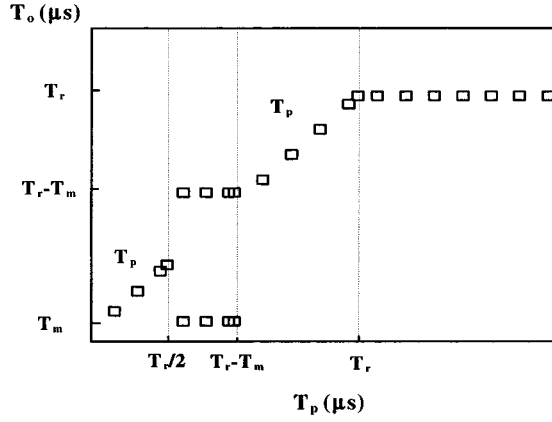


FIG. 3. Output periods as a function of the pacemaker period for long distances (30 circuits, $d=\lambda$). For $T_p > T_r$, the reentry dominates the rhythm of the medium. For $T_p \in [T_r - T_m, T_r]$, the pacemaker controls the rhythm of the medium. For $T_p \in (T_r/2, T_r - T_m)$, two output waves were observed ($T_1 = T_m = 110 \pm 2.5 \mu\text{s}$ and $T_2 = 220 \pm 2.5 \mu\text{s}$ following the sequence $T_1 T_2$ with $T_1 + T_2 = T_r$) as a result of the interaction. Finally, for $T_p \leq T_r/2$, the pacemaker dominates again.

on the medium as observed for longer distances. Two different output periods were obtained once again for $T_p \in (T_r/2, T_r - T_m)$ with the same values and following the same relation as for $T_p \geq T_r$. Finally, for $T_p \leq T_r/2$ the pacemaker dominates the reentry rhythm as obtained for longer distances.

For shorter distances $d < 1/3\lambda$ (Fig. 5), a more complicated interaction is observed. For $T_p > T_r$, the obtained multifrequency output waves follow the formula

$$\sum_{i=1}^N n_i T_i = m T_p, \quad (1)$$

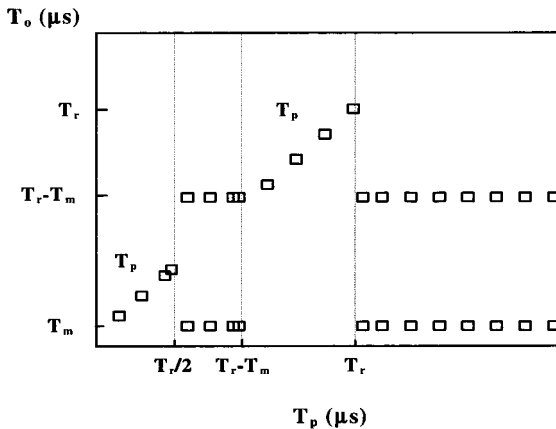


FIG. 4. Output periods as a function of the pacemaker period for intermediate distances (15 circuits, $d=\lambda/2$). For $T_p > T_r$ two output periods were observed ($T_1 = T_m = 110 \pm 2.5 \mu\text{s}$ and $T_2 = 220 \pm 2.5 \mu\text{s}$ following the sequence $T_1 T_2$ with $T_1 + T_2 = T_r$) as a result of the interaction between pacemaker and reentry. For $T_p \in [T_r - T_m, T_r]$ the pacemaker controls the rhythm of the medium. For $T_p \in (T_r/2, T_r - T_m)$ two output waves were observed once again with the same values and the same sequence as observed for $T_p > T_r$. Finally, for $T_p \leq T_r/2$ the pacemaker dominates again.

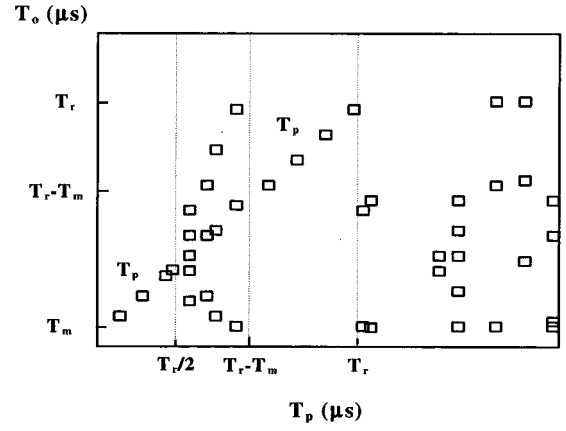


FIG. 5. Output periods as a function of the pacemaker period for short distances (5 circuits, $d=\lambda/6$). For $T_p > T_r$ multifrequency output waves were observed as a result of the interaction. For $T_p \in [T_r - T_m, T_r]$ the pacemaker controls the rhythm of the medium. For $T_p \in (T_r/2, T_r - T_m)$ a new region of multifrequency output waves was obtained and, finally, for $T_p \leq T_r/2$ the pacemaker dominates again.

where N is the number of different output periods in each sequence, n_i is the number of times that the period T_i appears in each sequence, and m an integer number verifying $\sum_{i=1}^N n_i > m$, in such a way that the mean period belongs to the interval $[T_r/2, T_r]$. This multifrequency behavior changes drastically for $T_p \in [T_r - T_m, T_r]$, where the pacemaker imposes its rhythm on the medium. For $T_p \in (T_r/2, T_r - T_m)$ a new multifrequency region appears. In this region, the different periods obey the expression (1) but with $\sum_{i=1}^N n_i = m$, in such a way that the mean period coincides with T_p . Finally, for $T_p \leq T_r/2$, the pacemaker dominates again, as observed for the rest of the distances.

V. NEARBY SOURCES

In order to characterize the complex multifrequency interaction between a reentry and a normal pacemaker in its proximity ($d < 1/3\lambda$) the following parameters were considered: $R_l = 2.3 \text{ k}\Omega$, $R_t = 4.7 \text{ k}\Omega$, $d = 0.27\lambda$, $T_r = 178.0 \pm 0.5 \mu\text{s}$, and $T_p/T_r > 1$. Note that for the obstacle considered, only a reentry can rotate in a stationary way around it. In this range, it is possible to obtain wave sequences in which two [Fig. 6(a)], three [Fig. 6(c)], and even more different frequencies are involved as a result of the competition between the autonomous pacemaker and the reentry ($T_r = 178.0 \pm 0.5 \mu\text{s}$). In Fig. 6(b), for $T_p = 322.2 \mu\text{s}$, two different output periods ($T_1 = 178.0 \pm 2.5 \mu\text{s}$, and $T_2 = 143.0 \pm 2.5 \mu\text{s}$) following the sequence $T_1 T_2$ were found. In Fig. 6(d), three different output periods $T_1 = 178.0 \pm 2.5 \mu\text{s}$, $T_2 = 140.0 \pm 2.5 \mu\text{s}$ and $T_3 = 167.0 \pm 2.5 \mu\text{s}$, following the sequence $(5T_1)T_2 T_3$ were observed for $T_p = 200 \mu\text{s}$. In general, for any $T_p/T_r > 1$, we have observed the appearance of experimental sequences $(nT_1)T_2 \dots T_{k+1-n}$, where, in every sequence, n is the number of times that the period $T_1 = T_r$ appears and $k+1$ the number of output waves. The response of the system to the periodic forcing obeys the formula

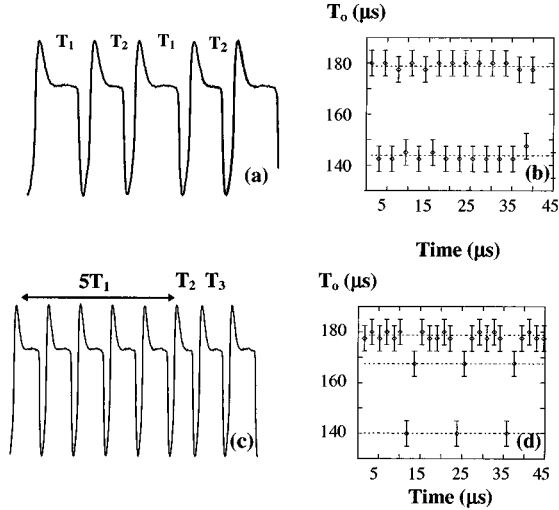


FIG. 6. Sequences of two and three different output periods generated by the interaction between a reentry ($T_r = 178.0 \pm 0.5 \mu\text{s}$) and a pacemaker located in its proximity. For $T_p = 322.2 \mu\text{s}$, two different output periods ($T_1 = 178.0 \pm 2.5 \mu\text{s}$, and $T_2 = 143.0 \pm 2.5 \mu\text{s}$) were found following the sequence $T_1 T_2$ as shown in (a) and (c) (voltage vs time plot). For $T_p = 200.0 \mu\text{s}$, three different output periods ($T_1 = 178.0 \pm 2.5 \mu\text{s}$, $T_2 = 140.0 \pm 2.5 \mu\text{s}$, and $T_3 = 167.5 \pm 2.0 \mu\text{s}$) were found following the sequence $(5T_1) T_2 T_3$ as shown in (b) and (d) (period vs time plot).

$$nT_1 + \sum_{i=2}^{k+1-n} T_i = \frac{(k-1)}{\text{int}(T_p/T_r)} T_p, \quad (2)$$

whose validity was experimentally checked for two and three different output periods. In fact, Eq. (2) can be explicitly solved when only two different output periods are considered:

$$T_2 = n \left(\frac{T_p}{\text{int}(T_p/T_r)} - T_r \right), \quad (3)$$

where n can be calculated assuming that $T_2 \in [T_m, T_r]$, and T_m is the refractory period of the medium as previously defined.

In this case, the firing numbers $[k+1:n+1]$ where $k+1$ is the number of output waves and $n+1$ the number of input (delivered) pulses] were calculated in the interval $T_p/T_r \in [1, 2)$ [Fig. 7(a)] for different T_p values, following a devil's staircase. Lines represent the theoretical period given by Eq. (3) and rhombi the measured experimental points. A similar behavior can be found for any $T_p/T_r > 2$, where each step in the devil's staircase is calculated following the expression $\text{int}(T_p/T_r)m+1:m$ with $m \geq 2$. Note that there are regions between two consecutive steps where Eq. (3) cannot be applied. These intervals correspond to the narrow zones where a two period sequence cannot be found and more complex behaviors with three or more different periods can be observed to follow the Farey tree sequence.

Values of T_2 as a function of the normal pacemaker period were represented [Fig. 7(b)] in the interval $T_p/T_r \in [1, 2)$. Lines represent the theoretical period given by Eq. (3) and rhombi the measured experimental points. Once

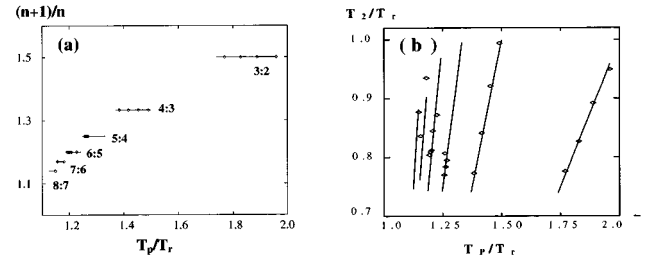


FIG. 7. Firing numbers and T_2/T_r in the interval $T_p/T_r \in [1, 2)$ obtained for a two output period sequence. In (a), the firing number (defined as $k+1:n+1$, where $k+1$ is the number of output waves and $n+1$ the number of input pulses) is observed to follow the devil's staircase. In (b), the normalized output period (T_2/T_r) is observed to decrease linearly along each step in the devil's staircase. In both plots, lines represent the prediction given by Eq. (3) and rhombi the experimental points. The intervals between consecutive steps correspond to the regions where Eq. (3) fails, in which sequences with more than two periods were experimentally observed.

again, a similar sequence can be observed for any T_p longer than T_r . The other period $T_1 = T_r$ was not plotted for the sake of clarity.

Different authors have considered circle maps [39–43] to describe the interaction between two sources [31,44,45] (a normal pacemaker and an ectopic one with slower period). The case we are considering has some particularly interesting features, namely, (1) the normal pacemaker (the external pulse generator) has a period slower than the ectopic one (the reentry); (2) the normal pacemaker is autonomous and cannot be reset by the reentry; (3) the reentry can be reset by the normal pacemaker in such a way that it annihilates the previous reentry and generates a new one; and (4) the distance between sources plays a key role in describing their interaction. A similar analysis can be carried out by means of the following iterative function.

$$\Phi_{i+1} = \begin{cases} (\Phi_i + \tau) \pmod{1}, & \text{if } 0 < (\Phi_i + \tau) \pmod{1} < \theta \\ \tau \pmod{1}, & \text{otherwise} \end{cases} \quad (4)$$

where $\tau = T_p/T_r$ and $\theta = T_m/T_r$. The first equation corresponds to the pacing stimulus falling within the refractory period of the reentry wave and causing no resetting. The second equation corresponds to the pacing stimulus falling outside the refractory period of the reentry wave and causing resetting of the reentry.

This linear analysis of the iteration between both sources predicts the appearance of the two-period sequences described in Fig. 7. Unfortunately, the characterization of a nonlinear function to fit the existence of more than two frequencies is beyond the scope of this experimental paper due to the inaccuracy in some of the time series obtained.

VI. CONCLUSIONS

In summary, we have obtained different output wave sequences depending on the distance between two wave sources (Fig. 8). Each sequence depends on the source that dominates the medium, whose rhythm can be imposed by a

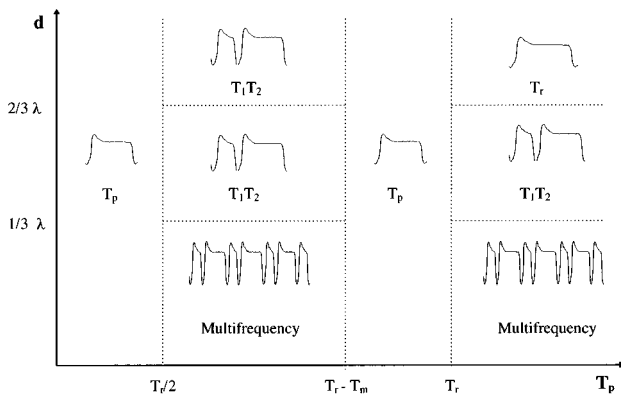


FIG. 8. Diagram of output sequences due to the interaction between a reentry and a pacemaker. A summary of the interaction is plotted as a function of distance between sources ($0 \leq d \leq \lambda$) and pacemaker period $T_p \in [T_m, 2T_r]$.

single pacemaker (the ectopic or the normal one) or by interaction between them.

For $T_p > T_r$, the sequence of output periods becomes more and more complicated when distance between both sources decreases. For long distances ($d \geq 2/3\lambda$), the stimuli delivered by the pulse generator (pacemaker) never reach the obstacle (they collide and annihilate with the waves generated by the reentry). The observed output period is always T_r .

For intermediate distances ($1/3\lambda < d < 2/3\lambda$), some properly timed stimulus is able to reach the obstacle and provoke phase resetting, in such a way that two waves can coexist, rotating around the obstacle in a stationary way. This gives rise to an effective (mean) period ($T_{\text{eff}} = T_r/2$), which prevents any further stimulus from reaching the obstacle.

Finally, for short distances ($d \leq 1/3\lambda$), the pacemaker is able to reset the reentry from time to time, even when its effective period is $T_r/2$. As a result of this interaction, a complex multiperiod output sequence is observed, with an effective period $T_{\text{eff}} \in [T_r/2, T_r]$. A similar behavior, where different frequencies are involved, has been described by other authors, but forcing the medium with a period shorter than the refractory period [15–17] or considering interaction between a normal pacemaker (T_p) and an ectopic one (T_r), where T_p is shorter than T_r [31]. In our experiments, when a stimulus delivered by the pacemaker arrives at the obstacle, it gives rise to a phase shift in the reentry as explained in Winfree's seminal book [1]. When the stimulus arrives after the refractory period of the previous reentry, it initiates a

premature wave, which prevents the next circulating pulse to propagate. In a certain way, this provokes phase resetting. When the stimulus arrives during the refractory period, it cannot propagate and only delays slightly the period of the next circulating pulse. This behavior depends on the different nature of both pacemakers, since the normal pacemaker is considered to be autonomous and cannot be reset. In addition, the presence of this pacemaker in the proximity of the reentry allows the stimuli coming from the pulse generator to reach the obstacle and to reset the reentry, even for $T_p > T_r$, as previously described.

This behavior changes for $T_p \in [T_r - T_m, T_r]$, where the pacemaker emits with a period faster than the one corresponding to the reentry. A wave rotating around the obstacle cannot complete the turn due to the refractory tail of the next pacemaker pulse. So, the reentry is never formed and the observed output period is T_p .

For $T_p \in [T_r/2, T_r - T_m]$, interaction between both sources is observed again. Now, the difference between T_r and T_p is big enough to allow some of the waves rotating around the obstacle to complete its turn. The dependence on the distance is similar to the one observed for $T_p > T_r$.

Finally, for $T_p \leq T_r/2$ ($T_r/2$ is the fastest effective period around the obstacle) the pacemaker dominates once again as shown for $T_p \in [T_r - T_m, T_r]$.

The observed sequence of periods can be predicted by means of the linear iterative function described in the previous section [Eq. (4)] at least for two period sequences. This linear function allows the autonomous pacemaker to either reset the reentry or to be blocked by the previous reentry. However, this external pacemaker cannot modify the refractoriness of the medium and does not predict the multifrequency sequences observed experimentally. To obtain this effect it is necessary to modify the previous model by adding nonlinear terms [43–45].

Throughout this paper we have characterized the influence of the distance on the interaction between a normal and an ectopic pacemaker. This is the first step in developing and implementing new defibrillation methods, which are now in progress [46].

ACKNOWLEDGMENTS

We want to thank Carlos Rico for his help with the experimental setup. This work was partially supported by the ‘Comisión Interministerial de Ciencia y Tecnología’ (Spain) under Project No. DGICYT-PB94-0623 and ‘Conselleria de Educación e Ordenación Universitaria, Xunta de Galicia’ (Spain) under Project No. XUGA 20602B97.

- [1] A. T. Winfree, *The Geometry of Biological Time* (Springer-Verlag, New York, 1980).
- [2] J. D. Murray, *Mathematical Biology* (Springer-Verlag, New York, 1989).
- [3] G. R. Mines, *Trans. R. Soc. Can.* **4**, 43 (1914).
- [4] T. Lewis, and A. M. Master, *Heart* **12**, 209 (1925).
- [5] *Mathematical Approaches to Cardiac Arrhythmias*, edited by

- J. Jalife, special issue of *Ann. N. Y. Acad. Sci.* **591** (1990).
- [6] *Theory of Heart*, edited by L. Glass, P. Hunter, and A. McCulloch (Springer, New York, 1991).
- [7] A. V. Panfilov and A. V. Holden, *Phys. Lett. A* **151**, 23 (1990).
- [8] M. Courtemanche and A. T. Winfree, *Int. J. Bifurcation Chaos Appl. Sci. Eng.* **1**, 431 (1991).
- [9] V. S. Zykov, *Simulation of Wave Processes in Excitable Media*

- (Manchester University Press, Manchester, 1987).
- [10] N. Wiener, and A. Rosenblueth, Arch. Inst. Cardiol. Mex. **16**, 205 (1946).
- [11] M. Courtemanche, L. Glass, and J. P. Keener, Phys. Rev. Lett. **70**, 2182 (1993); SIAM (Soc. Ind. Appl. Math.) J. Appl. Math. **56**, 119 (1996).
- [12] H. Ito and L. Glass, Physica D **56**, 84 (1992).
- [13] B. Braaksma and J. Grasman, Physica D **68**, 265 (1993).
- [14] M. Feingold, D. L. González, O. Piro, and H. Viturro, Phys. Rev. A **37**, 4060 (1988).
- [15] D. R. Chialvo and J. Jalife, Nature (London) **330**, 749 (1987).
- [16] D. R. Chialvo, R. F. Gilmore, Jr., and J. Jalife, Nature (London) **343**, 653 (1990).
- [17] H. Sevcikova and M. Marek, Physica D **49**, 114 (1991).
- [18] V. Pérez-Muñuzuri, M. Alonso, L. O. Chua, and V. Pérez-Villar, Int. J. Bifurcation Chaos Appl. Sci. Eng. **4**, 1631 (1994).
- [19] A. Toth, V. Gaspar, and K. Showalter, J. Phys. Chem. **98**, 522 (1994).
- [20] M. P. Kennedy, K. R. Krieg, and L. O. Chua, IEEE Trans. Circuits Syst. **36**, 1133 (1989).
- [21] J. Luprano and M. Hasler, IEEE Trans. Circuits Syst. **36**, 146 (1989).
- [22] A. P. Muñuzuri, M. Gómez-Gesteira, V. Pérez-Muñuzuri, V. I. Krinsky, and V. Pérez-Villar, Phys. Rev. E **48**, 3232 (1993); **50**, 4258 (1994); Int. J. Bifurcation Chaos Appl. Sci. Eng. **4**, 1245 (1994).
- [23] M. Ruiz-Villarreal, M. Gómez-Gesteira, C. Souto, A. P. Muñuzuri, and V. Pérez-Villar, Phys. Rev. E **54**, 2999 (1996).
- [24] M. Ruiz-Villarreal, M. Gómez-Gesteira, and V. Pérez-Villar, Phys. Rev. Lett. **78**, 779 (1997).
- [25] V. I. Krinsky and K. L. Agladze, Physica D **8**, 50 (1983).
- [26] O. Steinbock and S. C. Müller, Int. J. Bifurcation Chaos Appl. Sci. Eng. **3**, 437 (1993).
- [27] I. P. Mariño, M. deCastro, V. Pérez-Muñuzuri, M. Gómez-Gesteira, L. O. Chua, and V. Pérez-Villar, IEEE Trans. Circuits Syst. **42**, 665 (1995).
- [28] M. deCastro, V. Pérez-Muñuzuri, I. P. Mariño, M. Gómez-Gesteira, L. O. Chua, and V. Pérez-Villar, Int. J. Bifurcation Chaos Appl. Sci. Eng. **6**, 1725 (1996).
- [29] A. T. Winfree, Physica D **49**, 125 (1991).
- [30] I. S. Aranson, L. Kramer, and A. Weber, Physica D **53**, 376 (1991); Phys. Rev. Lett. **67**, 404 (1991); Phys. Rev. E **47**, 3231 (1993).
- [31] M. Courtemanche, L. Glass, J. Bélair, D. Scagliotti, and D. Gordon, Physica D **40**, 299 (1989).
- [32] R. N. Madan, *Chua's Circuit: A Paradigm for Chaos*, World Scientific Series of Nonlinear Science, Ser. B1 (World Scientific, Singapore, 1993).
- [33] A. P. Muñuzuri, V. Pérez-Muñuzuri, M. Gómez-Gesteira, L. O. Chua, and V. Pérez-Villar, Int. J. Bifurcation Chaos Appl. Sci. Eng. **5**, 17 (1995).
- [34] V. Pérez-Muñuzuri, A. P. Muñuzuri, M. Gómez-Gesteira, V. Pérez-Villar, L. Pivka, and L. O. Chua, Philos. Trans. R. Soc. London, Ser. A **353**, 101 (1995).
- [35] V. Pérez-Muñuzuri, V. Pérez-Villar, and L. O. Chua, Int. J. Bifurcation Chaos Appl. Sci. Eng. **2**, 403 (1992).
- [36] J. P. Keener, SIAM (Soc. Ind. Appl. Math.) J. Appl. Math. **47**, 556 (1987); J. Theor. Biol. **148**, 49 (1991).
- [37] J. Brugada *et al.*, Circulation **81**, 1633 (1990).
- [38] M. A. Allesie *et al.*, Eur. Heart J. **10**, 8 (1990).
- [39] L. Glass and R. Pérez, Phys. Rev. Lett. **48**, 26 (1982).
- [40] T. Geisel and J. Nierwetberg, Phys. Rev. Lett. **48**, 1 (1982).
- [41] M. Schell, S. Fraser, and R. Kapral, Phys. Rev. A **28**, 1 (1983).
- [42] D. Rand, S. Ostlund, J. Sethna, and E. Siggia, Phys. Rev. A **49**, 2 (1982).
- [43] J. Bélair and L. Glass, Physica D **16**, 143 (1985).
- [44] L. Glass, M. Guevara, J. Bélair, and A. Shrier, Phys. Rev. A **29**, 3 (1984).
- [45] M. Guevara, L. Glass, and A. Shrier, Science **214**, 18 (1981).
- [46] M. deCastro, M. Gómez-Gesteira, H. Zhang, and V. Pérez-Villar, Phys. Rev. E **57**, 949 (1998).